5. Nucleation Dynamics

5.1 Homogeneous Nucleation
of Liquid Droplet and Vapor Bubble

5.2 Heterogeneous Nucleation
of Liquid Droplet and Vapor Bubble

5.3 Generation of Special Structures

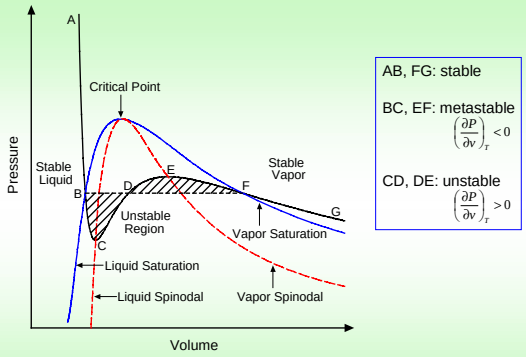

Thermodynamic limit of superheat

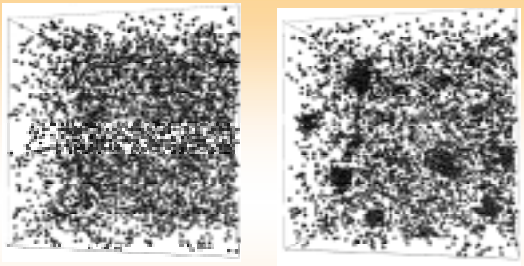

Yasuoka & Matsumoto (1998)

Homogeneous Nucleation

Heterogeneous Liquid Droplet Nucleation on Solid Surface

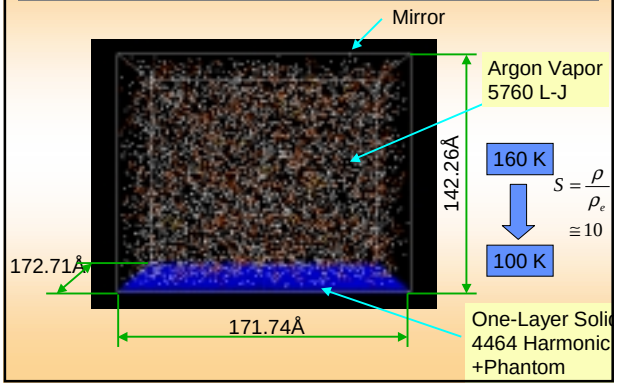

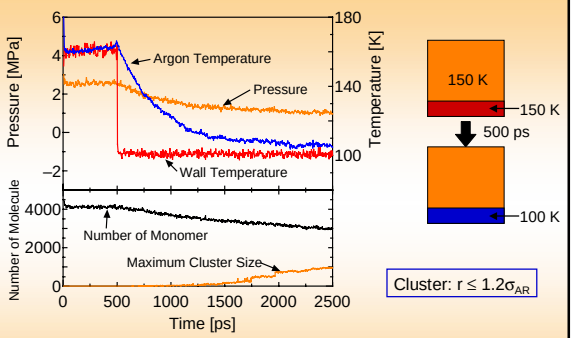

Pressure, temperature, number of monomer and maximum cluster size variations (E2)

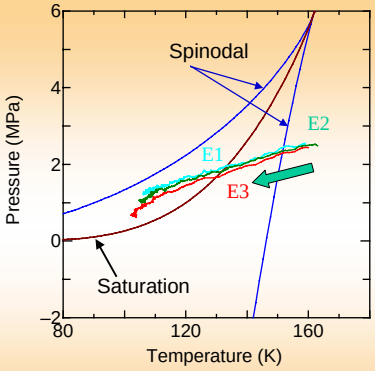

Pressure-Temperature Diagram

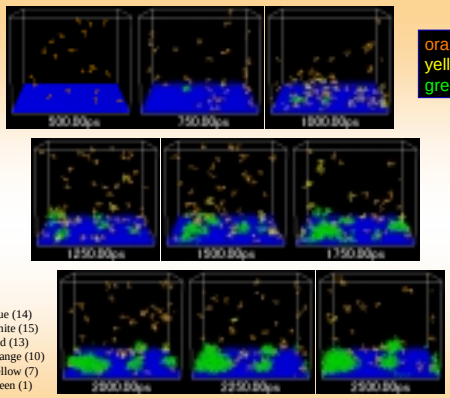

Snapshots of cluster larger than 5 atoms (E2)

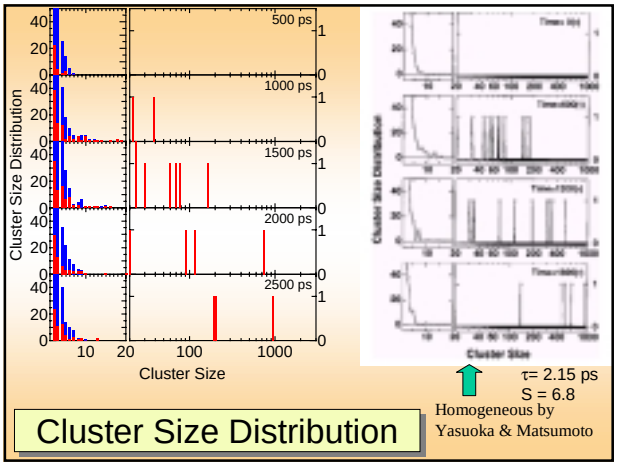

Cluster Size Distribution

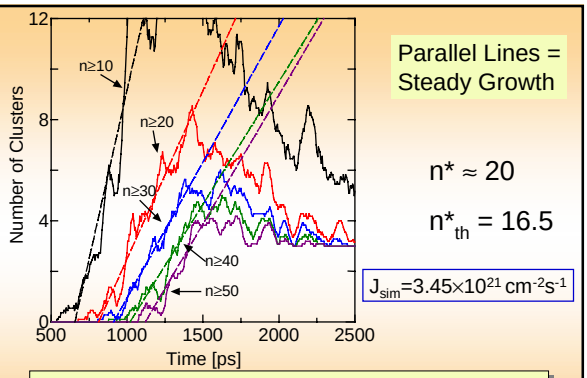

Parallel Lines = Steady Growth

$n^* \approx 20$

$n^*_{th} = 16.5$

$J_{sim}=3.45\times10^{21}\ cm^{-2}s^{-1}$

Number of Clusters Larger than Threshold

Critical Radius & Free Energy

Area $A = 4\pi r^2$ Volume $V = \frac{4}{3}\pi r^3$

Surface tension γ

Free Energy of Cluster $\Delta G = \gamma A + \Delta g V$

Free energy difference
In solid and vapor for unit volume
Assumption of ideal gas $\Delta g = -\rho_l k_B T \ln(\frac{\rho}{\rho_e})$

Number of molecules $n = \rho_l V$

Supersaturation Ratio $S = \frac{\rho}{\rho_e}$

$r^* = \frac{2\gamma}{\rho_l k_B T \ln S}$ $n^* = \frac{32\pi\gamma^3 f}{3\rho_l^2 (k_B T \ln S)^3}$ $\Delta G^* = \frac{16\pi\gamma^3 f}{3(\rho_l k_B T \ln S)^2}$

Heterogeneous nucleation from plane solid surface

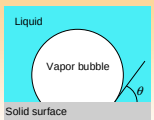

$$J = N^{\frac{2}{3}}\left(\frac{1+\cos\theta}{2}\right)\sqrt{\frac{2\sigma_{lv}}{\pi m B f(\theta)}}\exp\left(-\frac{16\pi\sigma_{lv}^3 f(\theta)}{3kT(\eta P_{SAT}(T)-P)^2}\right)$$

$$B = 1-\frac{1}{3}\left(1-\frac{P}{\eta P_{SAT}(T)}\right)\approx\frac{2}{3},\quad \eta = \exp\frac{v(P-P_{SAT}(T))}{RT},\quad f(\theta)=\frac{1}{4}(2+3\cos\theta-\cos^3\theta)$$

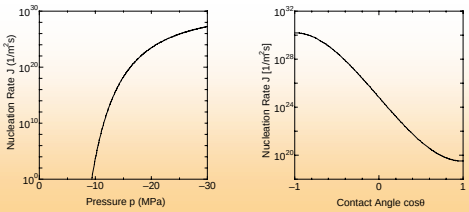

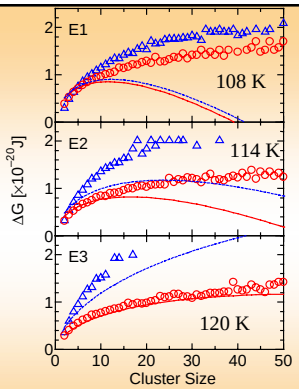

Blue: Homogeneous
Red: Heterogeneous

Symbols: Estimation from cluster distribution c(n)
Valid until Critical Size

$c(n) = \rho^{\frac{2}{3}} \exp\left(-\frac{\Delta G}{k_B T}\right)$

Lines: Classical Theory

$\Delta G = \left(4\pi r^2\gamma - \frac{4}{3}\pi r^3 \rho_l k_B T \ln S\right) f$

$n = \frac{4}{3}\pi r^3 \rho_l f$

Gibb's Free Energy

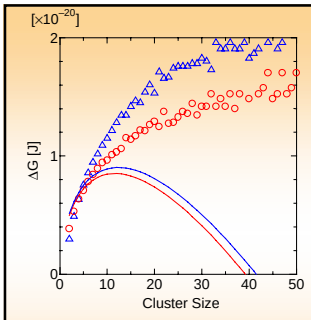

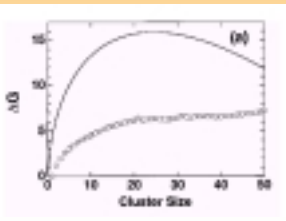

Homogeneous
Yasuoka & Matsumoto (1998)

E1: less wettable

Comparison of Free Energy

Calculation Conditions and Nucleation Rates

Label	ε_{INT} [$\times 10^{-21}$ J]	θ [deg]	T_{ave} [K]	J_{sim} [$cm^{-2}s^{-1}$]	J_{th} [$cm^{-2}s^{-1}$]
E1	0.426	135.4	108	6.52×10^{20}	48.6×10^{20}
E2	0.612	105.8	114	34.5×10^{20}	44.7×10^{20}
E3	0.798	87.0	120	57.6×10^{20}	5.54×10^{20}

Simulated

Classical Theory

Yasuoka & Matsumoto:
Homogeneous MD: J_{sim} was 7 orders larger than J_{th}

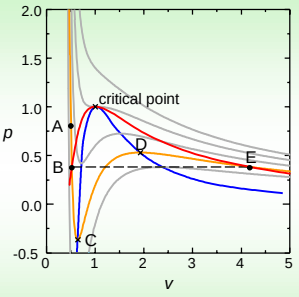

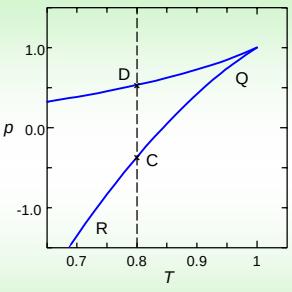

Isotherm of van der Waals

spinodal line

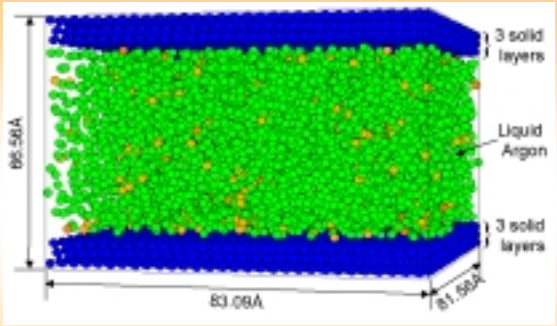

A snapshot of liquid argon between parallel solid surfaces

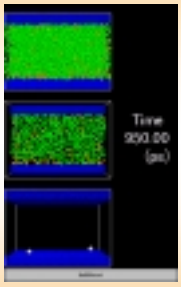

Nucleation of Vapor on Solid Surface

Slice View

pv

Void View

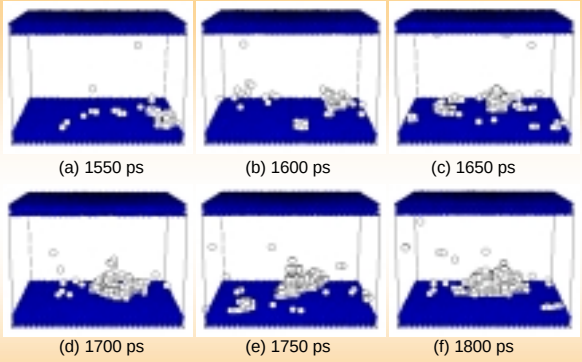

(a) 1550 ps (b) 1600 ps (c) 1650 ps

(d) 1700 ps (e) 1750 ps (f) 1800 ps

Snapshots of void patterns for P3

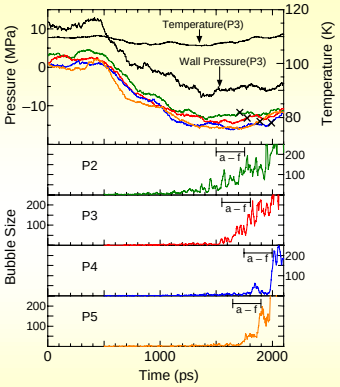

Pressure, temperature and bubble size variations

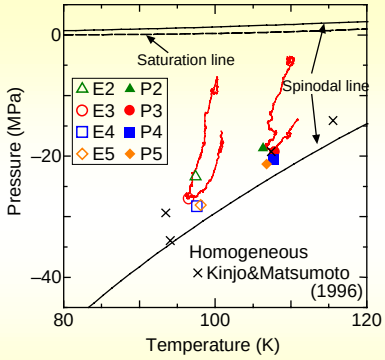

wettable surface
↓
need higher superheat to nucleate

Pressure and temperature variations and spinodal line

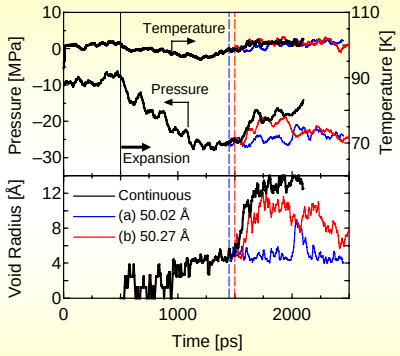

500～1000 ps
等温体積弾性率
B_T=-V($\partial p/\partial V$)$_T$=257 MPa

気泡半径
20.7 Å
↓
圧力上昇
Δp=-B_T($\Delta V/V$)=7.7 MPa

Nucleation process by stopping expansion at certain point

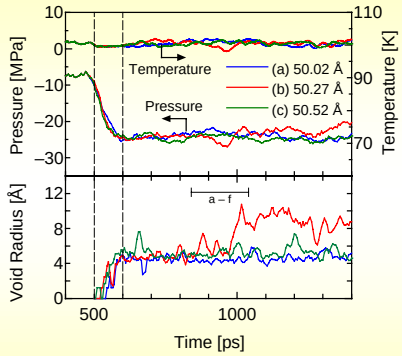

気泡核成長の待ち時間
τ=400 ps
↓
核生成速度
J_{MD}=3.7×10^{21} cm^{-2}s^{-1}

最大ボイド半径
8 Å
↓
臨界気泡核半径
10-15 Å

Nucleation process by stopping expansion at certain point

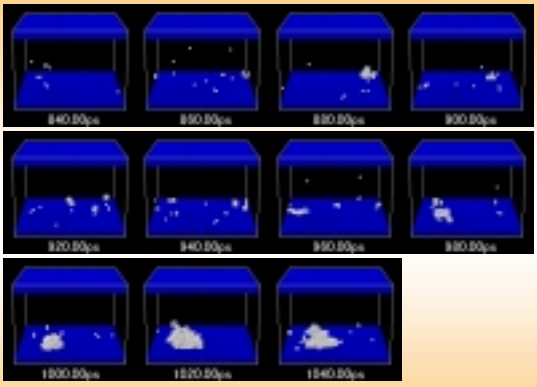

Time history of void pattern (h=50.27Å)

Heterogeneous nucleation from plane solid surface

$$J = N^{\frac{2}{3}}\left(\frac{1+\cos\theta}{2}\right)\sqrt{\frac{2\sigma_{lv}}{\pi m B f(\theta)}}\exp\left(-\frac{16\pi\sigma_{lv}^{3} f(\theta)}{3kT(\eta p_{sat}(T)-p)^{2}}\right)$$

$$B=1,\quad \eta=\exp\frac{v(p-p_{sat}(T))}{RT},\quad f(\theta)=\frac{1}{4}(2+3\cos\theta-\cos^{3}\theta)$$

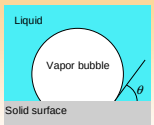

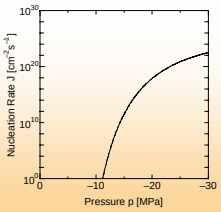

$$r_e=\frac{\eta p_{sat}(T)-p}{2\sigma_{lv}}$$

T =100 K
p =-23.8 MPa → J_{TH}=2.0×10^{20} cm^{-2}s^{-1}, r_e=7.9 Å
θ=68°

J_{MD}= 3.7×10^{21} cm^{-2}s^{-1}

Comparison with Classical Theory

Classical Theory: $J = 2.0 \times 10^{20}$ cm^{-2}s^{-1}, r_e = 7.9 Å

Waiting Time τ = 400 ps

$J = 1/(A\,\tau) = 3.7 \times 10^{21}$ cm^{-2}s^{-1} ?

Void Radius 8 Å, Limit of Rapid Growth

cf. 均質核生成（T. Kinjo & M. Matsumoto, 1998)

J_{MD}=1.53×10^{29} cm^{-3}s^{-1}

J_{TH}=4.23×10^{21} cm^{-2}s^{-1}

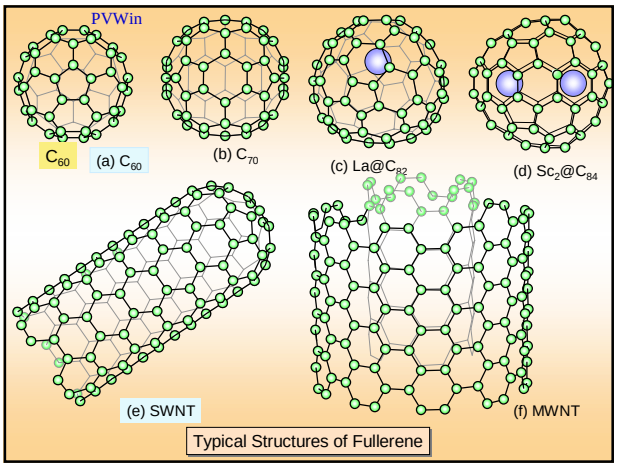

Typical Structures of Fullerene

Total Energy E_b:

$$E_b = \sum_i \sum_{j(<i)} \{V_R(r_{ij}) - B^*_{ij} V_A(r_{ij})\}$$

$$V_R(r) = f(r)\frac{D_e}{S-1}\exp\{-\beta\sqrt{2S}(r-R_e)\} \qquad V_A(r) = f(r)\frac{D_e S}{S-1}\exp\left\{-\beta\sqrt{\frac{2}{S}}(r-R_e)\right\}$$

$$B^*_{ij} = \frac{B_{ij}+B_{ji}}{2}, \quad B_{ij} = \left[1+\sum_{k(\neq i,j)}\{G_c(\theta_{ijk})\,f(r_{ik})\}\right]^{-\delta}$$

$$G_c(\theta) = a_0\left(1+\frac{c_0^2}{d_0^2}-\frac{c_0^2}{d_0^2+(1+\cos\theta)^2}\right)$$

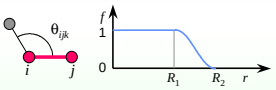

Cut-off function

Potential parameters

D_e =	6.325 eV	S =	1.29	β =	1.5Å^{-1}	R_e =	1.315Å
δ =	0.80469	a_0 =	0.011304	c_0 =	19	d_0 =	2.5
R_1 =	1.7Å	R_2 =	2.0Å				

From D. W. Brenner: *Phys. Rev. B*, **42**, 9458(1990)

C-C Potential Function

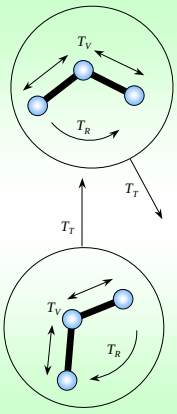

$$\bar{\mathbf{r}} = \frac{1}{n}\sum_{i=1}^{n}\mathbf{r}_i, \quad \mathbf{r}_i' = \mathbf{r}_i - \bar{\mathbf{r}} \qquad \bar{\mathbf{v}} = \frac{1}{n}\sum_{i=1}^{n}\mathbf{v}_i, \quad \mathbf{v}_i' = \mathbf{v}_i - \bar{\mathbf{v}}$$

$$\Rightarrow \begin{cases} K_T = \frac{1}{2}nm|\bar{\mathbf{v}}|^2 \\ K_R = \frac{\left|\sum_{i=1}^{n} m\mathbf{r}_i' \times \mathbf{v}_i'\right|^2}{2\sum_{i=1}^{n} m|\mathbf{r}_i'|^2} \\ K_V = \frac{1}{2}\sum_{i=1}^{n} m|\mathbf{v}_i'|^2 - K_R \end{cases}$$

$$T_T = \frac{2K_T}{3k_B} \qquad T_T^{\text{total}} = \frac{\sum \nu_T T_T}{\sum \nu_T} = \frac{2\sum K_T}{3Nk_B}$$

$$T_R = \frac{2K_R}{k_B \nu_R} \qquad T_R^{\text{total}} = \frac{\sum \nu_R T_R}{\sum \nu_R} = \frac{2\sum K_R}{k_B \sum \nu_R} \Rightarrow T_c$$

$$T_V = \frac{2K_V}{k_B \nu_V} \qquad T_V^{\text{total}} = \frac{\sum \nu_V T_V}{\sum \nu_V} = \frac{2\sum K_V}{k_B \sum \nu_V}$$

Temperature Control

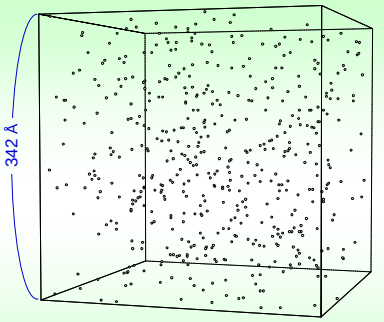

Randomly distributed 500 carbon atoms with random velocities

Control temperature T_c = 3000 K

Calculating Conditions

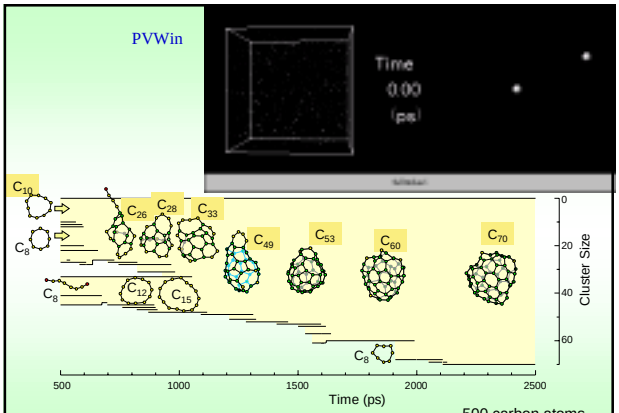

Growth Process

500 carbon atoms
342 Å cubic box
T_c = 3000 K

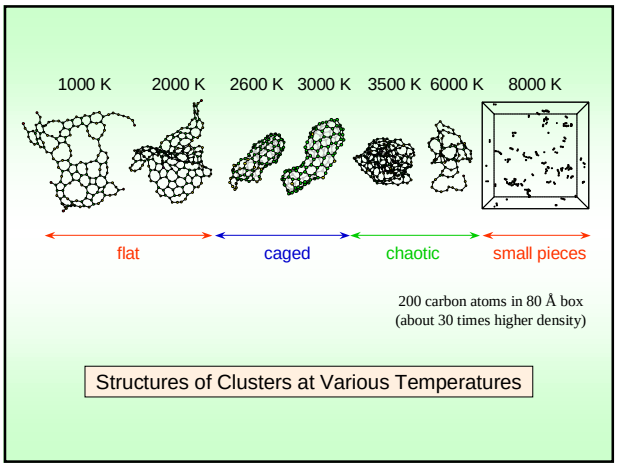

Structures of Clusters at Various Temperatures

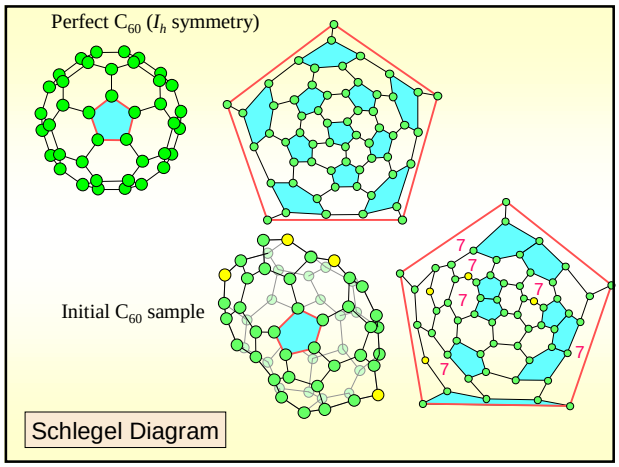

Schlegel Diagram

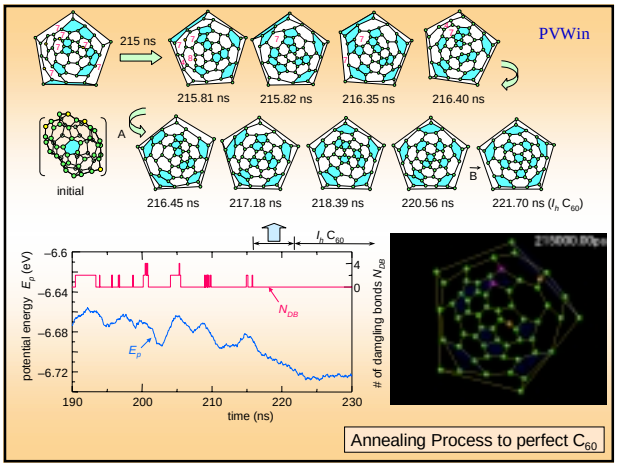

Annealing Process to perfect C_{60}

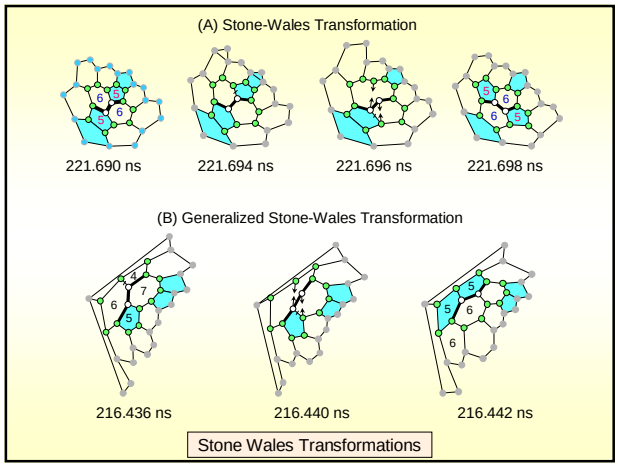

Stone Wales Transformations

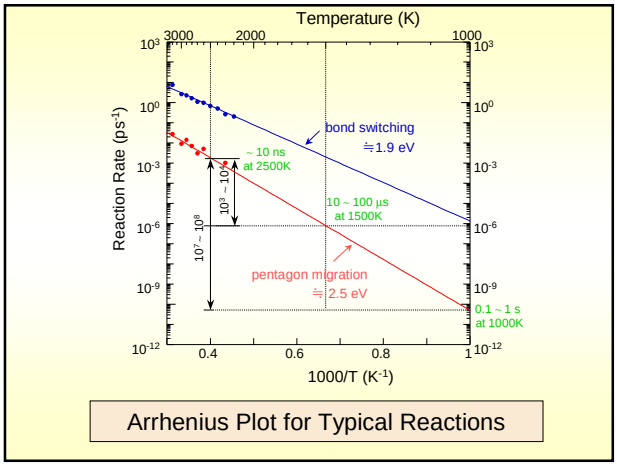

Arrhenius Plot for Typical Reactions

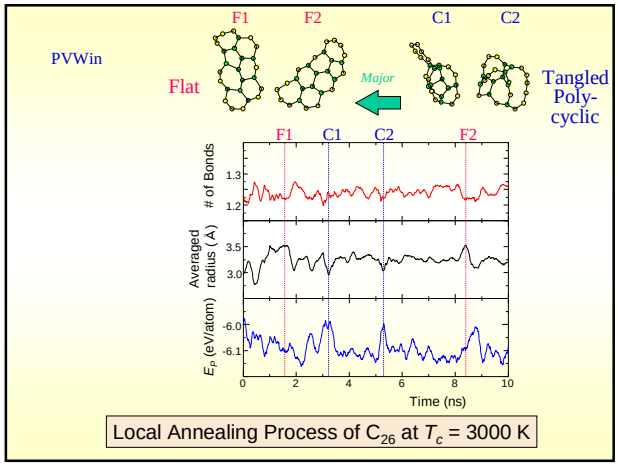

Local Annealing Process of C_{26} at T_c = 3000 K

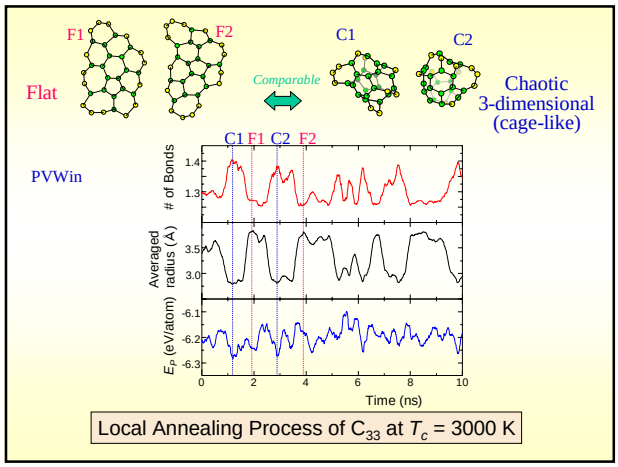

Local Annealing Process of C_{33} at T_c = 3000 K

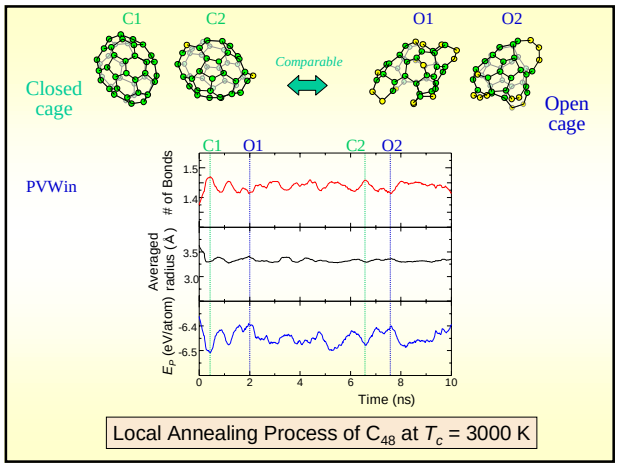

Local Annealing Process of C_{48} at T_c = 3000 K

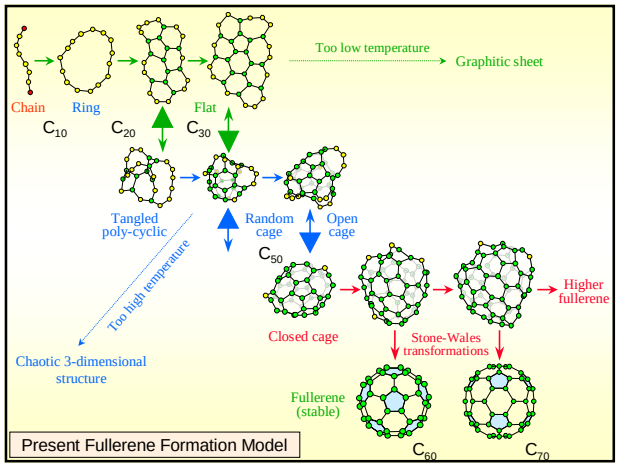

Present Fullerene Formation Model

Group	1	2	3	4	5	6	7	8	9	10	11	12	13	14	15	16	17	18
Period																		
1	1 H 1.008																	2 He 4.003
2	3 Li 6.941	4 Be 9.012											5 B 10.81	6 C 12.01	7 N 14.01	8 O 16.00	9 F 19.00	10 Ne 20.18
3	11 Na 22.99	12 Mg 24.31											13 Al 26.98	14 Si 28.09	15 P 30.97	16 S 32.07	17 Cl 35.45	18 Ar 39.95
4	19 K 39.10	20 Ca 40.08	21 Sc 44.96	22 Ti 47.88	23 V 50.94	24 Cr 52.00	25 Mn 54.94	26 Fe 55.85	27 Co 58.93	28 Ni 58.69	29 Cu 63.55	30 Zn 65.39	31 Ga 69.72	32 Ge 72.61	33 As 74.92	34 Se 78.96	35 Br 79.90	36 Kr 83.80
5	37 Rb 85.47	38 Sr 87.62	39 Y 88.91	40 Zr 91.22	41 Nb 92.91	42 Mo 95.94	43 Tc 99.00	44 Ru 101.1	45 Rh 102.9	46 Pd 106.4	47 Ag 107.9	48 Cd 112.4	49 In 114.8	50 Sn 118.7	51 Sb 121.8	52 Te 127.6	53 I 126.9	54 Xe 131.3
6	55 Cs 132.9	56 Ba 137.3	*	72 Hf 178.5	73 Ta 180.9	74 W 183.8	75 Re 186.2	76 Os 190.2	77 Ir 192.2	78 Pt 195.1	79 Au 197.0	80 Hg 200.6	81 Tl 204.4	82 Pb 207.2	83 Bi 209.0	84 Po 210.0	85 At 210.0	86 Rn 222.0
7	87 Fr 223	88 Ra 226	**	104 Unq 261	105 Unp 262	106 Unh 263	107 Uns 262	108 Uno 265	109 Une 266	110 Uun 269	111 Uuu 272	112 Uub 277						
=																		
* Lanthanides			57 La 138.9	58 Ce 140.1	59 Pr 140.9	60 Nd 144.2	61 Pm 145	62 Sm 150.4	63 Eu 152	64 Gd 157.3	65 Tb 158.9	66 Dy 162.5	67 Ho 164.9	68 Er 167.3	69 Tm 168.9	70 Yb 173.0	71 Lu 175.0	
** Actinides			89 Ac 227	90 Th 232	91 Pa 231	92 U 238	93 Np 237	94 Pu 239	95 Am 243	96 Cm 247	97 Bk 247	98 Cf 252	99 Es 252	100 Fm 257	101 Md 258	102 No 259	103 Lr 262	

Studied Metal Atoms

$E_{ij} = V_R + V_A + V_C$

$f(r_{ij})$: cut-off function

V_R: Repulsive term

$$V_R = f(r_{ij})\frac{D_e}{S-1}\exp\left\{-\beta\sqrt{2S}(r_{ij}-R_e)\right\}$$

V_A: Attractive term

$$V_A = -f(r_{ij})\cdot B^*\frac{D_eS}{S-1}\exp\left\{-\beta\sqrt{2/S}(r_{ij}-R_e)\right\}$$

M-C

B^*: normalized bond order

$$B^* = \left\{1+b(N^C-1)\right\}^{\delta}$$

N^C: carbon coordinate number

$$N^C = 1+\sum_{\text{carbon } k(\neq j)} f(r_{ik})$$

V_C: Coulomb term

$$V_C = -f(r_{ij})\frac{e^2}{4\pi\varepsilon_0}\frac{c_C c_M}{r_{ij}}$$

M-M

$$R_e(N_{ij}) = R_{e1} - R_{e2}\exp\left\{-C_R(N_{ij}-1)\right\}$$

$$D_e(N_{ij}) = D_{e1} + D_{e2}\exp\left\{-C_D(N_{ij}-1)\right\}$$

$N^M{}_i$: metal coordinate number

$$N^M{}_i = 1+\sum_{\text{metal } k(\neq j)} f(r_{ik}) \qquad N_{ij} = \frac{N^M{}_i + N^M{}_j}{2}$$

$$V_C = f(r_{ij})\frac{e^2}{4\pi\varepsilon_0}\frac{c_{Mi}c_{Mj}}{r_{ij}}$$

c_M, c_C : charge of M (+) and C(-)

$$c_M = 3-\exp(-k_1N^C+k_2) \qquad c_C = c_M/N^C$$

M-C and M-M Potential Function Expression

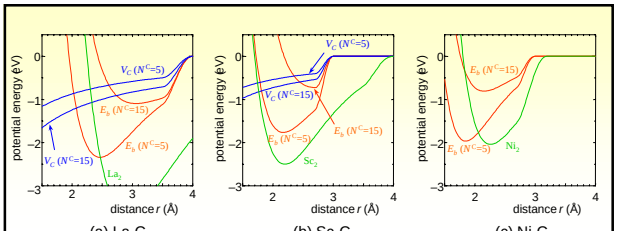

Table 1. Potential parameters for metal-carbon interactions.

	D_e (eV)	S	β (1/Å)	R_e (Å)	R_1 (Å)	R_2 (Å)	b	δ	k_1	k_2
La-C	4.53	1.3	1.5	2.08	3.2	3.5	0.0854	-0.8	0.0469	1.032
Sc-C	3.82	1.3	1.7	1.80	2.7	3.0	0.0936	-0.8	0.0300	1.020
Ni-C	3.02	1.3	1.8	1.70	2.7	3.0	0.0330	-0.8	–	–

Table 2. Potential parameters for metal-metal interactions.

	S	β (1/Å)	D_{e1} (eV)	D_{e2} (eV)	C_R	R_{e1} (Å)	R_{e2} (Å)	C_D	$R_{1,1}$ (Å)	$R_{2,1}$ (Å)
La-La	1.3	1.05	0.740	2.64	0.570	3.735	0.777	0.459	4.0	4.5
Sc-Sc	1.3	1.4	0.645	1.77	0.534	3.251	0.919	0.620	3.5	4.0
Ni-Ni	1.3	1.55	0.74	1.423	0.365	2.520	0.304	0.200	2.7	3.2

Metal-Carbon Potential functions

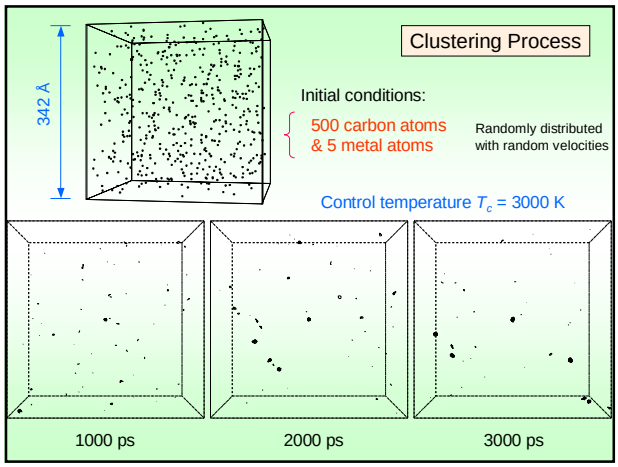
Clustering Process
342 Å
Initial conditions:
500 carbon atoms
& 5 metal atoms
Randomly distributed
with random velocities
Control temperature T_c = 3000 K
1000 ps
2000 ps
3000 ps

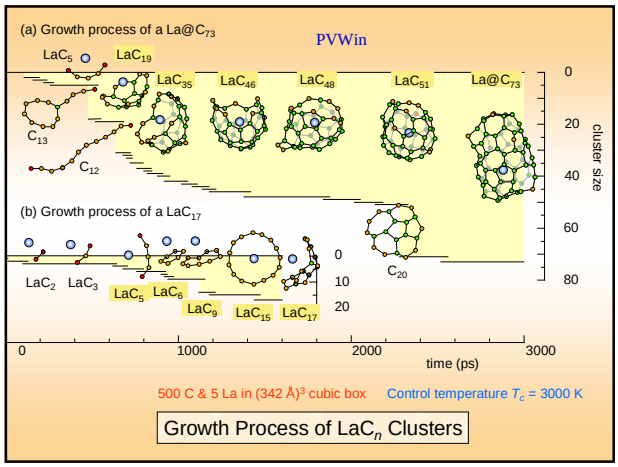
(a) Growth process of a La@C73
PVWin
LaC5
LaC19
LaC35
LaC46
LaC48
LaC51
La@C73
C13
C12
(b) Growth process of a LaC17
LaC2
LaC3
LaC5
LaC6
LaC9
LaC15
LaC17
C20
cluster size
time (ps)
500 C & 5 La in (342 Å)3 cubic box
Control temperature T_c = 3000 K
Growth Process of LaC$_n$ Clusters

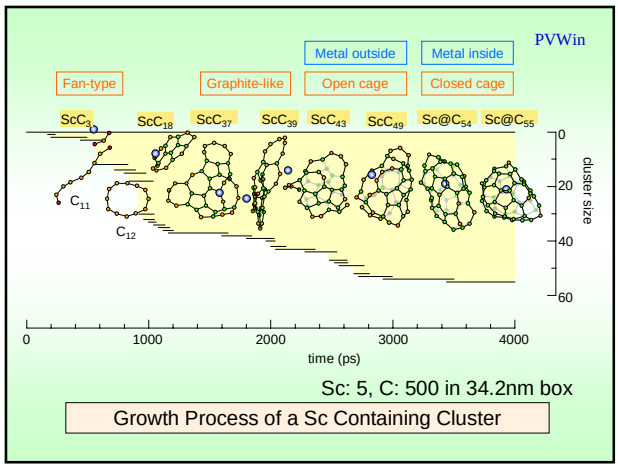
PVWin
Metal outside
Metal inside
Fan-type
Graphite-like
Open cage
Closed cage
ScC3
ScC18
ScC37
ScC39
ScC43
ScC49
Sc@C54
Sc@C55
C11
C12
cluster size
time (ps)
Sc: 5, C: 500 in 34.2nm box
Growth Process of a Sc Containing Cluster

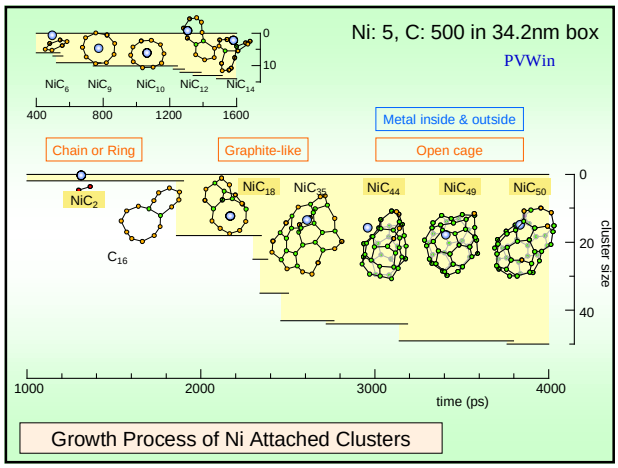
Ni: 5, C: 500 in 34.2nm box
PVWin
NiC6
NiC9
NiC10
NiC12
NiC14
Metal inside & outside
Chain or Ring
Graphite-like
Open cage
NiC2
NiC18
NiC35
NiC44
NiC49
NiC50
C16
cluster size
time (ps)
Growth Process of Ni Attached Clusters

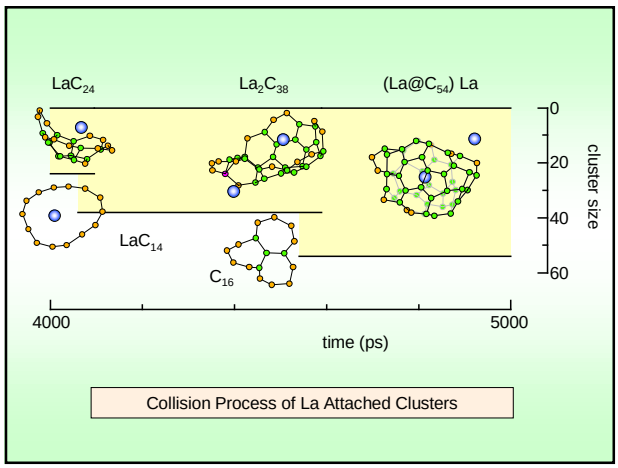
LaC24
La2C38
(La@C54) La
LaC14
C16
cluster size
time (ps)
Collision Process of La Attached Clusters

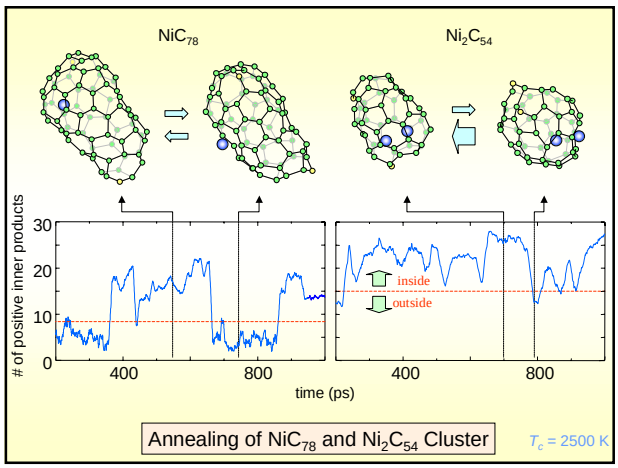
NiC78
Ni2C54
# of positive inner products
inside
outside
time (ps)
Annealing of NiC78 and Ni2C54 Cluster
T_c = 2500 K